JOURNAL OF CATALYSIS **163,** 176–185 (1996)
ARTICLE NO. 0317

Selective Sulfur Dioxide Adsorbents Prepared from Designed Dispersions of Groups IA and IIA Metal Oxides on Alumina

S. N. R. Rao,* E. Waddell,† M. B. Mitchell,† and Mark G. White*

*Focused Research Program in Surface Science and Catalysis; *School of Chemical Engineering, Georgia Institute of Technology, Atlanta, Georgia 30332-0100; and †Department of Chemistry, Clark Atlanta University, Atlanta, Georgia 30310*

Received May 23, 1995; revised May 6, 1996; accepted May 28, 1996

Supported M(I)/alumina and M(II)/alumina adsorbents were prepared using $M^{n+}(acac)_n$ as the precursor. These materials may be decomposed by careful heating to create dispersions of $M^{n+}O_{n/2}$/alumina which are SO_2 adsorbents. These adsorbents have been characterized by elemental analyses, diffuse reflectance infrared Fourier transform analysis spectroscopy, SO_2 adsorption capacity, and powder X-ray diffraction. The MgO/alumina prepared from $Mg(acac)_2 \cdot 2H_2O$ shows high dispersion of Mg species which are stable against sintering even when calcined to 500°C. The incremental SO_2 sorption capacity of this material shows nearly 1 mol SO_2/mol Mg^{2+} in the sample. The sample prepared from Li(acac) shows more SO_2 adsorption than the MgO/alumina for loadings <150 μmol/g alumina. However, the LiO/alumina samples show low incremental adsorption of SO_2 per mol of Li ion (0.12 mol/mol) at metal loadings greater than 150 μmol/g alumina. These results are discussed in the framework of ensemble theory in the light of the solution chemistry of the metal acetylacetonates.

INTRODUCTION

Among all of the pollutants, particulate matter (dust) and sulfur oxides (SO_2 and SO_3) have received special attention from researchers as these pollutants account for most of the environmental and health problems faced today (1). Almost all of the SO_2 and SO_3 emissions are the result of the combustion of sulfur-containing fuels or elemental sulfur. Attention has been focused on the reduction of emissions from coal-fired power plants since these emission were 70% of the total in 1966.

The present technology for abatement of sulfur dioxide emissions is the limestone process where the sulfur is sequestered in the form of a solid sulfate. This technology exchanges an air pollution problem for a solid disposal problem. The present study focuses on a reversible adsorption technique for recovering the sulfur dioxide. The pollutant is concentrated into a gas stream of low volumetric flow rate relative to the original flue gas which may be sold as is or reconstituted into another form of sulfur for sale as a product.

Background Literature

The current SO_2 adsorbents are alumina (Al_2O_3) which have been promoted either with an alkali (2) or a transition metal ion such as Cu (3). Catalysts for SO_x reduction include the magnesium aluminate spinel (4). We limit the discussion to γ-aluminas which have been promoted by alkali and alkaline metal ions.

Surface chemistry of γ-alumina. The surface of γ-alumina shows a rich variety of surface structures to include up to five different types of OH groups (5). "Pure" alumina catalyzes several reactions (6–10), some of which demand acidic sites and others which demand basic surface sites. From this perspective then, alumina is said to show both acid and base sites.

Models of the surface have been developed from defect-free crystals of Al_2O_3 which were cut to expose the desired crystal face (11–13). These models show OH groups attached to Al ions in tetrahedral coordination (T_d) and octahedral coordination (O_h) and explain, qualitatively, the known IR spectrum. Knözinger explains the acidic and basic properties of the OH groups as a consequence of the charge residing on these groups (13). Moreover, the models can simulate the dehydroxylation of the surface which is observed upon heating of the alumina. We use the models here in a general manner to understand the adsorption of SO_2.

The conventional models for SO_2 adsorption on alumina show that Lewis base (electron donor) and a Brønsted base (labile OH group) are used (14–19). The most popular mechanism (Scheme I) involves the initial chemisorption of SO_2 at a Lewis acid site (structure **I** or **II**), or at a Lewis base site (structure **III**) with the eventual oxidation at high temperature (400°C) to the sulfate (structure **VI**) (16, 17). Structure **III** may lose an oxygen from the surface and subsequently rearrange to form structure **I**. Two other forms of sorbed SO_2 were assigned to structures **IV** and **V**. Structure **V** was a hydrogen-bonded form of chemisorbed SO_2, whereas structure **IV** was attributed to physisorbed SO_2. In this connection the adsorption of SO_2 to alumina

0021-9517/96 $18.00

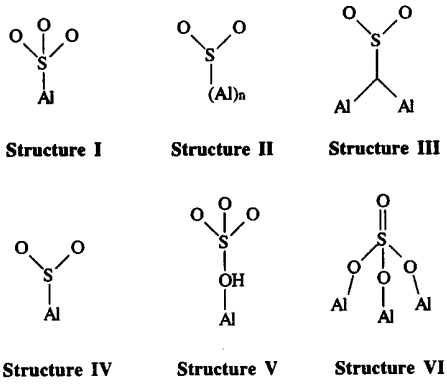

SCHEME I

is attended by electron-pair donation from the lone pair of the sulfur to an electron acceptor such as a coordinately unsaturated site on an Al^{3+} to form structures **I**, **II**, or **IV**. The other form of chemisorbed SO_2 shows the donation of an electron pair from the surface oxygen (Lewis base) into the electron-acceptor state of the sulfur to produce structures **III** or **V**.

Promotion of γ-alumina. The adsorption properties of the alumina may be improved with the addition of other metals to its surface such as alkali and alkaline earths. The effects of the alkali/alkaline may be direct—new sites for SO_2 adsorption are created—or indirect by enhancing the chemisorption properties of the sites already present on the surface of the alumina. A direct effect for adding the alkali is that the alkali ions (M^{n+}) become new sites to chemisorb the SO_2 as shown in the following equation:

$$M^{n+}(OH)_n \text{ (solid)} + SO_2 \text{ (gas)} \rightarrow M^{n+}(OH)_nSO_2 \text{ (solid)}.$$

Thus, the effect of adding alkali is to increase the number of chemisorbing sites assuming that the alkali does not block sites on the alumina which sorb SO_2.

The additon of alkali to the surface may increase the SO_2 adsorption in an indirect manner by changing the electronic environment of the alumina surface, e.g., increase the net negative charge on the O or OH groups as a result of electron transfer from the alkali to the O or OH oxygen. This effect would result in increasing the SO_2 adsorption by donating electrons from the alkali atoms to the basic O or OH groups so as to improve the ability to donate electrons to the SO_2 as in structures **III** and **V**. The addition of alkali to the surface may improve the Lewis acidity of the coordinately unsaturated site on an Al^{3+} either by dehydrating the surface or by withdrawing electron density from the Al ions. The former may be accomplished by association with the alkali metals ions, whereas the latter is realized only by reaction with the alkali to form another species such as a spinel which increases the number of octahedrally coordinated Al ions (20).

Use of metal acetylacetonates. We have demonstrated the usefulness of metal acetylacetonates as precursors in preparing supported metal oxides (21). Kenvin showed that $Cu(acac)_2$ was anchored to silica as a result of hydrogen bonding between the surface OH and the complex (21). The supported CuO/silica was prepared by careful heating of the monolayer of $Cu(acac)_2$. The resulting CuO apparently resisted sintering to maintain a high dispersion of the metal ions even when heated to 450°C.

These results suggest that the different types of OH groups on the alumina may also engage in hydrogen-bonding to the $Mg(acac)_2$ molecule. We speculate that the $Mg(acac)_2$ molecule will selectively attach to the acidic OH groups leaving the basic OH groups free to adsorb SO_2 (13). If the $Mg(acac)_2$ molecule anchors to the surface of alumina in the same way that $Cu(acac)_2$ became affixed to the surface of silica, then a fine dispersion of MgO is expected to result from thermolysis of a monolayer of $Mg(acac)_2$ on alumina which resist sintering upon heating to the decomposition temperature of the $Mg(acac)_2$ molecule.

Other metal ions which are stronger bases, such as those in group IA, may improve the adsorption capacity of the decorated alumina. The chemistry of acetylacetonates suggest that group IA metal acetylacetonate complexes are ionic and thus dissociate in solution. For example, White (22) showed that sodium and potassium acetylacetonates in ethanol are conductors of electricity, which suggests that these compounds dissociate in ethanol. However, the compounds did not completely dissociate at infinite dilution. Li(acac) is the least ionic in group IA and thus it is the most probable candidate to remain partially associated in solution. Another sample will be prepared from Li(acac) to describe the effect of group IA vs group IIA metal ions supported on the surface of alumina.

EXPERIMENTAL

Chemicals

The alumina used in this study was the γ-phase supplied by Goodfellows Corporation (Malvern, PA). The chemical assay showed Al_2O_3: 99.995% with the following trace impurities: Si, 8 ppm; Na, 3 ppm; Cu, 3 ppm; and Fe, 8 ppm. They reported a BET surface area of 148 m^2/g which compared favorably to the surface area which was reported by Micromeretics, Inc., for a sample of the material (153 m^2/g).

The metal acetylacetonates, $Mg(acac)_2 \cdot 2H_2O$ and Li(acac), were purchased from Strem Chemicals (Newburyport, MA). Methanol and acetonitrile were supplied by Fisher Chemical (Fair Lawn, NJ). Nitrogen (extra dry grade, 99.995% N_2) and oxygen (zero grade) were purchased from HOLOX (Atlanta, GA). The sulfur dioxide gas mixture (0.22% SO_2, balance N_2) were prepared by Matheson Gas Products (Morrow, GA).

Preparation of Adsorbents

Nonaqueous solvents were employed using metal acetylacetonates as the source of the alkali and alkaline metal ions. $Mg(acac)_2 \cdot 2H_2O$ was only sparingly soluble in methanol, whereas, Li(acac) was soluble in methanol. A batch impregnation was used to prepare adsorbents containing Li and for those with loadings of Mg < 74 μmol Mg/g Al_2O_3. Measured quantities of the metal complex were dissolved in 50 cm^3 of methanol. This solution was added to 10 g of alumina in 200 cm^3 of methanol and the mixture was stirred at room temperature for 10 h. The solids were separated from the liquid in a Buchner funnel and the retained solids were washed three times with 100 cm^3 aliquots of methanol. The washed solids were transferred to a vacuum drying oven which was held at 80°C and 5 inches Hg absolute pressure.

A Soxhlet extractor was used to prepare the adsorbents having loadings of $Mg(acac)_2 \cdot 2H_2O > 74$ μmol Mg/g Al_2O_3. The desired amount of metal acetylacetonate was put in the "thimble" of the extractor. Ten grams of alumina in 300 cm^3 of methanol was taken in a round-bottom flask and the contents were heated until all of the $Mg(acac)_2 \cdot 2H_2O$ was dissolved, which may require 48 h when high weight loading of the complex are desired. The solids were separated from the liquid in a Buchner funnel and the retained solids were washed three times with 100 cm^3 aliquots of methanol. The washed solids were transferred to a vacuum drying oven which was held at 80°C and 5 inches Hg absolute pressure.

Conductivity Tests

Tests were developed to determine, qualitatively, the dissociation of the metal acetylacetonates in solution. A YSI Model 32 conductivity meter was used to measure the electrical conductivity of the metal acetylacetonate solutions. Li(acac) was dissolved in methanol with a concentration of 0.4 *M*. The conductivity of the pure solvent was measured as the "blank." Standards include the strongly dissociating ionic solid ($LiClO_4$) and a strongly chelating metal complex [$Cu(acac)_2$].

Elemental Analyses

The samples were analyzed for metal (Applied Testing Services, Marietta, GA) and carbon content (Atlantic Microlabs, Inc., Norcross, GA). The results were the average of two tests to determine the metals analyses: ICP atomic emission and AA.

Thermogravimetric Analysis (TGA)

A description of the apparatus has been published earlier (23). Individual flows of N_2 and SO_2 (2200 ppm in N_2) were adjusted to produce a SO_2 concentration of 1100 ppm at a combined gas flow rate of 150 cm^3/min. Small amounts of the adsorbent (2–5 mg) were used to minimize the effects of exothermic heats of adsorption. A linear heating rate of 10–20°C/min was used in all tests. Pretreatment of the samples involved heating the sample from 25 to 500°C at 10°C/min in N_2 followed by cooling back to room temperature. The samples were exposed to the SO_2-laden gas for 20 min at room temperature and then purged for 20 min in N_2 only.

X-ray Diffraction

Powder X-ray diffraction (XRD) studies were completed on some samples to characterize the dispersion of the alkali/alkaline oxide in the sample. Large crystallites (>100 Å) would be obvious by appearance of XRD reflections. A physical mixture was prepared of alumina and $Mg(acac)_2 \cdot 2H_2O$ containing 1 wt% Mg to document the detection limit of the analysis. A Phillips PW1800 X-ray diffractometer was used in these experiments. The samples were scanned over a 2θ range of 5° to 60° in step sizes of 0.025° and an exposure time of 0.5 s. The irradiated sample length was 10 mm using an automatic divergence slit. The settings for the X-ray generator was 40 kV at 30 mA.

Diffuse Reflectance Infrared Fourier Transform Analysis Spectroscopy (DRIFTS)

Selected samples were analyzed for infrared active relaxations in a Nicolet 5DXB FTIR spectrometer. The IR spectra of these samples were used to infer the chemistry of the metal acetylacetonate and its interaction with the surface (21). The resolution of the instrument was 4 cm^{-1} and 2000 scans were averaged to develop each spectrum. Powder samples were ground and sieved then mixed with KBr so that a 5 wt% sample in KBr was prepared. The sample interferograms were compared against an interferogram of pure KBr and the data were converted to absorbance spectra using the Kubelka–Munk transform technique.

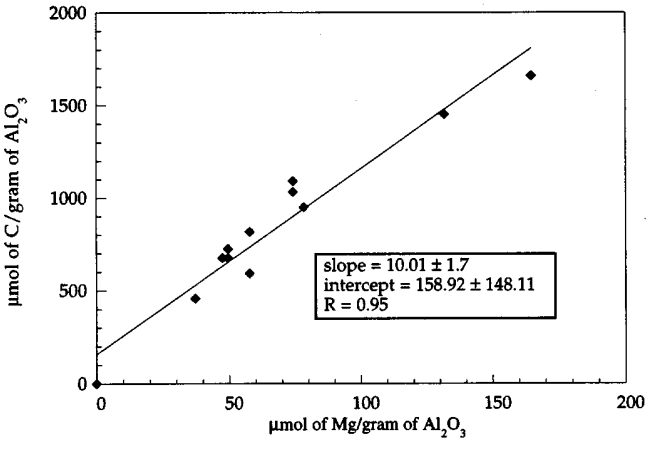

FIG. 1. Elemental analyses of $Mg(acac)_2/\gamma$-alumina.

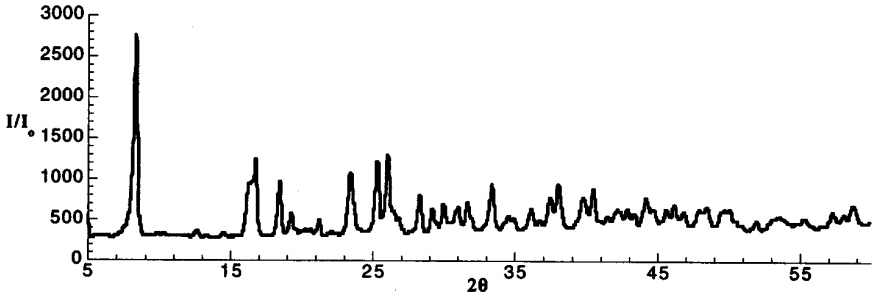

FIG. 2. Powder X-ray diffraction of neat $Mg(acac)_2 \cdot 2H_2O$.

RESULTS

Mg/Alumina

Samples of $Mg(acac)_2 \cdot 2H_2O$/alumina were examined for elemental analyses, XRD, DRIFTS, TGA of thermal decomposition, and SO_2 adsorption.

Elemental analyses. Samples prepared from $Mg(acac)_2 \cdot 2H_2O$ showed Mg loadings from 37 to 165 μmol Mg/g alumina and C loadings of 458 to 1658 μmol C/g alumina. Repeated attempts were unsuccessful for preparing supported magnesium samples with loadings greater than 165 μmol Mg/g alumina. This maximum loading corresponds to 41% of that estimated for a monolayer coverage on the alumina. A blank alumina sample which had experienced the same impregnation protocol without the metal complex showed 342 μmol C/g alumina. These data were plotted to determine the C/Mg stoichiometry (Fig. 1). A least-distance cruve fit showed a slope of 10.01 $\pm$ 0.73 mol C/mol Mg and an intercept of 158 $\pm$ 66 μmol C/g alumina. These data suggest that the C/Mg stoichiometry in the impregnated alumina is no different from that of the pristine metal complex (C/Mg = 10).

Powder XRD. The XRD of neat $Mg(acac)_2 \cdot 2H_2O$ shows the strongest reflection at 8.45° (d-spacing of 10.456 Å) with smaller peaks at 23.5° and 25.4° (Fig. 2). A mechanical mixture of $Mg(acac)_2 \cdot 2H_2O$ and alumina (1 wt% Mg) shows a peak at 8.45° and two small peaks at 23.5° and 25.5° (Fig. 3). This test documents the detection limit for crystallites of $Mg(acac)_2 \cdot 2H_2O$ on alumina. The γ-alumina shows only three large, broad peaks at 37°, 39°, and 46° (Fig. 4a). Two samples of $Mg(acac)_2 \cdot 2H_2O$/alumina (0.95 wt% Mg, 37 μmol Mg/g alumina, and 4.3 wt% Mg, 165 μmol Mg/g alumina) show no evidence of crystalline $Mg(acac)_2 \cdot 2H_2O$ (Figs. 4b, 4c).

DRIFTS. The diffuse reflectance IR of $Mg(acac)_2 \cdot 2H_2O$ and the dehydrated sample are shown in Fig. 5 (a, hydrate; b, sample a heated to 140°C). Apparently, heating the sample removes the waters of hydration as indicated by the decrease in size of peaks at 1470, 1590, 1648, and 1670 cm^{-1}. The spectrum (Fig. 5b) of the anhydrous $Mg(acac)_2$ shows peaks at 1615, 1525, 1475, 1410, and 1363 cm^{-1} which are similar to the peak locations reported by Lawson (24) (1629, 1534, 1490, 1422, 1374 cm^{-1}). Supported $Mg(acac)_2 \cdot 2H_2O$ (Fig. 6) show a spectrum similar to that of the dehydrated $Mg(acac)_2$, suggesting that the waters of hydration are lost upon contacting the alumina support. It is clear that the (acac) ligands are present in the supported sample. Some have suggested that related divalent (acac) complexes, e.g., $MoO_2(acac)_2$, react with alumina to anchor the MoO_2 to the surface with the (acac) ligands becoming affixed to the Al^{3+} ion as a surface bound $Al(acac)_2^+$ (25). We see no evidence of $Al(acac)_3$ in the DRIFT spectra as a major relaxation from the Al complex is not present in the spectra of the supported samples (24). Taken together the DRIFTS and stoichiometry data confirm that the $Mg(acac)_2$ becomes affixed to the surface of the alumina without the loss of (acac) ligands but the hydrates are probably lost.

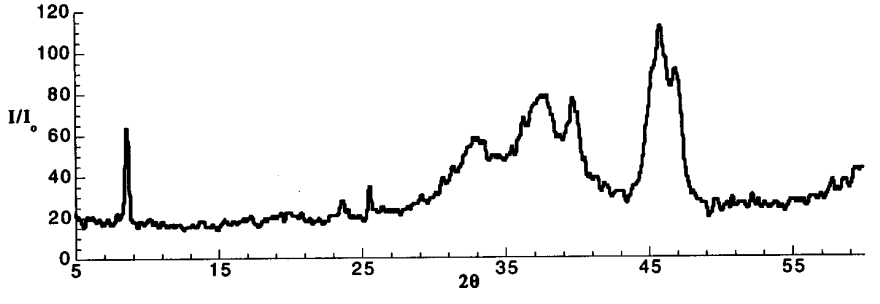

FIG. 3. Powder X-ray diffraction of a physical mixture of $Mg(acac)_2 \cdot 2H_2O$ and γ-alumina.

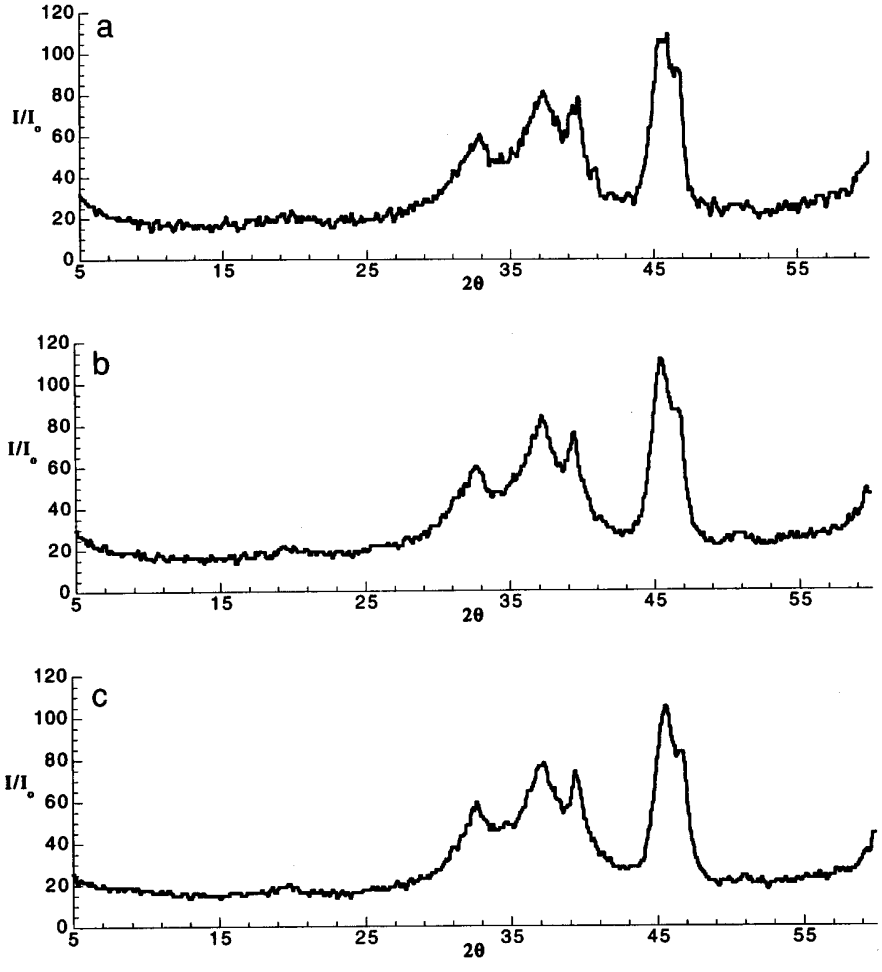

FIG. 4. Powder X-ray diffraction of $Mg(acac)_2/\gamma$-alumina. (a) γ-alumina; (b) 33.7 μmol $Mg(acac)_2$/g Al_2O_3; (c) 167 μmol $Mg(acac)_2$/g Al_2O_3.

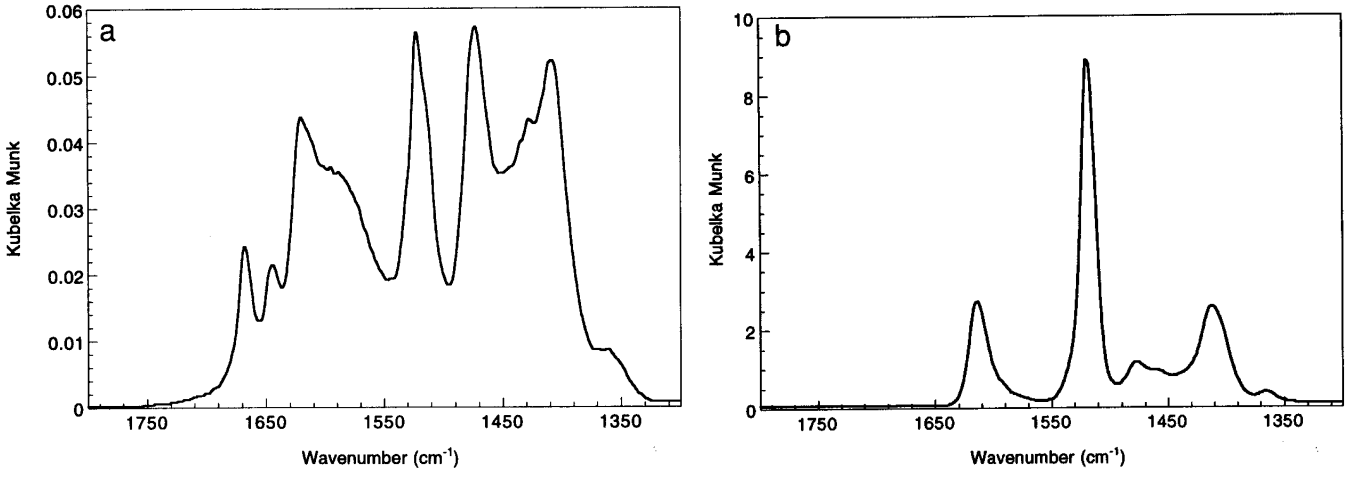

FIG. 5. Diffuse reflectance infrared Fourier transform spectroscopy of neat $Mg(acac)_2 \cdot 2H_2O$. (a) $Mg(acac)_2 \cdot 2H_2O$; (b) $Mg(acac)_2 \cdot 2H_2O$ heated to 140°C.

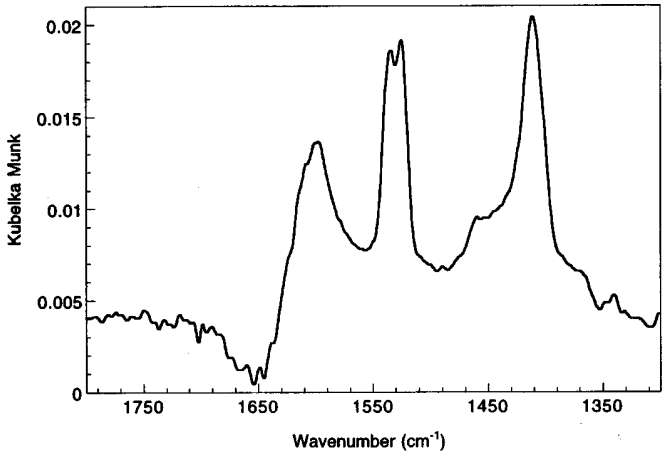

FIG. 6. Diffuse reflectance infrared Fourier transform spectroscopy of $Mg(acac)_2/\gamma$-alumina.

It is important to acknowledge the similarities and differences between the spectra of the anhydrous $Mg(acac)_2$ reported here and the $Cu(acac)_2$ reported by Kenvin (21) and Mitchell (26). Although similar in structure, the IR spectra of these two complexes differ in the number and location of the IR active peaks. The double-overtone deformation of the ring-carbon hydrogen (fundamental near 781 cm^{-1}, Ref. 24) is present in the $Cu(acac)_2$ spectrum at 1553 cm^{-1}. However, the fundamental of this deformation appears in the $Mg(acac)_2$ spectrum at 768 cm^{-1} which places the overtone of this relaxation at 1536 cm^{-1} (24). Therefore, we speculate that this overtone appears in the higher-frequency shoulder of the peak at 1525 cm^{-1} for the polycrystalline sample. This overtone peak becomes obvious in the supported sample (Fig. 6) at the expected frequency of 1536 cm^{-1}. The relaxations appear at similar frequencies for the asymmetric "breathing" of the carbon ring, the asymmetric and symmetric deformations of the methyl groups, and the asymmetric stretch for the carbonyl groups in the two molecules. However, the frequency is higher for the symmetric stretch for the carbonyl group in the $Mg(acac)_2$ than what is observed for $Cu(acac)_2$ (i.e., 1615 cm^{-1} vs 1576 cm^{-1}).

TGA—thermal decomposition. Thermal analysis of neat $Mg(acac)_2 \cdot 2H_2O$ when heated in oxygen shows the loss of two waters per mol of complex at temperatures between 80 and 100°C and the loss of one (acac) ligand between 220 and 280°C and the other (acac) ligand to form MgO between 420 and 480°C (Fig. 7). The overall weight loss is predicted within 1–2% assuming the following stoichiometry:

$$Mg(acac)_2 \cdot 2H_2O(s) \xrightarrow{\Delta} MgO(s) + \text{volatiles}.$$

The stepwise loss of the (acac) ligands has been observed for other metal acetylacetonates which form dimers and trimers in the crystal phase (27). The thermal analysis of supported $Mg(acac)_2$ on alumina revealed a spectrum not unlike that of "bare" alumina for which the features characteristic of metal complex decomposition are hidden under a spectrum of alumina dehydration.

TGA—SO_2 adsorption. The uptake of SO_2 was documented by thermogravimetry at room temperature under a flowing stream of SO_2/N_2 (1100 ppm SO_2). Bare alumina retained 265 μmol SO_2/g alumina for which all could be reversibly desorbed upon heating to 500°C. Samples of Mg-decorated alumina developed by thermolysis of the $Mg(acac)_2 \cdot 2H_2O$ show increasing amounts of SO_2 adsorption with increasing amount of Mg (Fig. 8). These data were fit by a least-difference routine to develop a slope of 0.92 mol SO_2/mol Mg and an intercept of 247 μmol SO_2/g alumina. This result suggests that the incremental SO_2 adsorption is close to the stoichiometry of 1 SO_2/Mg ion. Thus, we conclude that the Mg ions in this samples are well dispersed. The intercept is only 6.8% less than the SO_2 pick-up on bare alumina.

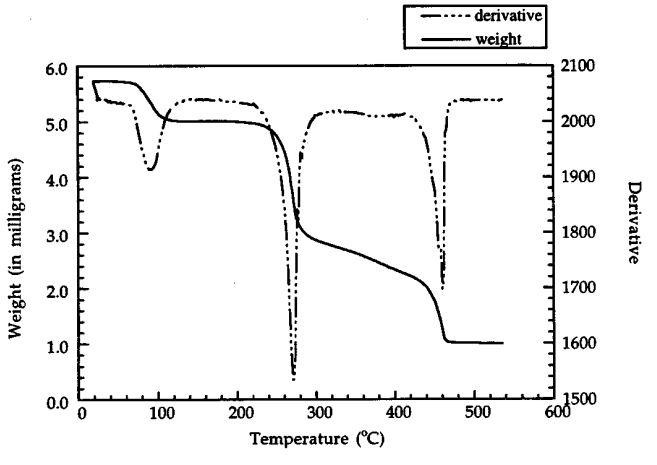

FIG. 7. Thermal gravimetric analysis of neat $Mg(acac)_2 \cdot 2H_2O$.

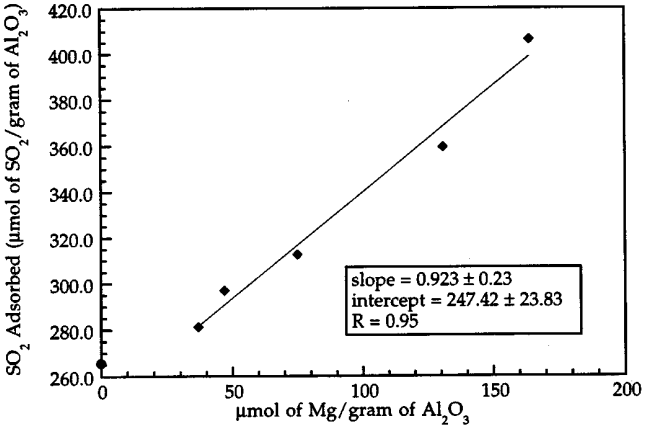

FIG. 8. SO_2 adsorption on $Mg(acac)_2/\gamma$-alumina.

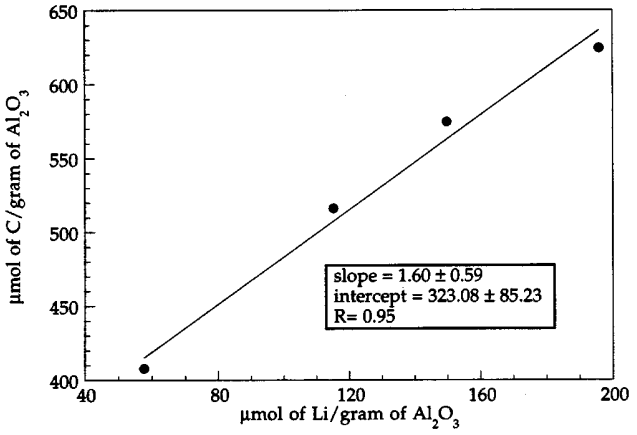

FIG. 9. Elemental analyses of Li(acac)/γ-alumina.

Li/Alumina

The adsorbents developed from Li(acac) on alumina were analyzed for elemental analyses, XRD, DRIFTS, TGA of thermal decompositions, and SO_2 adsorption. In addition, we documented qualitatively the extent of ionization of the Li(acac) in solution.

Electrical conductivity. Our initial data suggest that some of the Li(acac) is ionized in that the electrical conductivity of the MeOH solution (0.73 $\mu\Omega^{-1}$) increases by three orders magnitude when Li(acac) is solvated (2130 $\mu\Omega^{-1}$) at a concentration of 377 μmol/cm^3. The ionization may not be complete as $LiClO_4$ shows an increase in conductivity of another half-order of magnitude (8800 $\mu\Omega^{-1}$) at a concentration of 376 μmol/cm^3. The completely chelated $Cu(acac)_2$ shows a conductivity of 185 $\mu\Omega^{-1}$ at a concentration of 153 μmol/cm^3. These data are only qualitative in that the conductivity is determined by the mobility of all the ions in addition to the concentrations of the ions in solution.

Elemental analysis. Samples prepared from Li(acac) showed Li loadings from 58 to 196 μmol Li/g alumina and C loadings of 408 to 620 μmol C/g alumina. A blank alumina sample which had experienced the same impregnation protocol without the metal complex showed 342 μmol C/g alumina. These data were plotted to determine the C/Li stoichiometry (Fig. 9). A least-distance curve fit showed a slope of 1.6 mol C/mol Li and an intercept of 323 μmol C/g alumina. These data suggest that the C/ Mg stoichiometry in the impregnated alumina is much less than that of the pristine metal complex (C/Li = 5), which confirms the conductivity data that some of the complexes dissociated upon solvation. The intercept data suggest that some of the solvent may be retained by certain sites on the surface of the alumina perhaps by the same sites known to adsorb alcohol as reported by others (28).

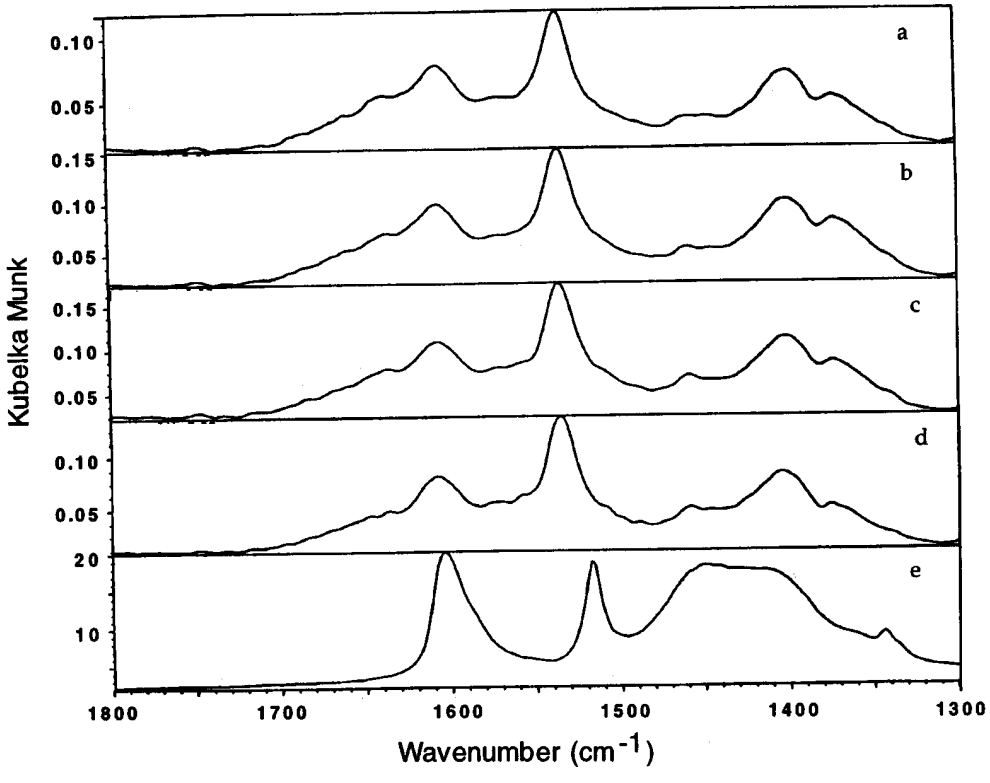

FIG. 10. Diffuse reflectance infrared Fourier transform spectroscopy of Li(acac)/γ-alumina. (a) 58 μmol Li(acac)/g Al_2O_3; (b) 115 μmol Li(acac)/g Al_2O_3; (c) 150 μmol Li(acac)/g Al_2O_3; (d) 196 μmol Li(acac)/g Al_2O_3; (e) neat Li(acac).

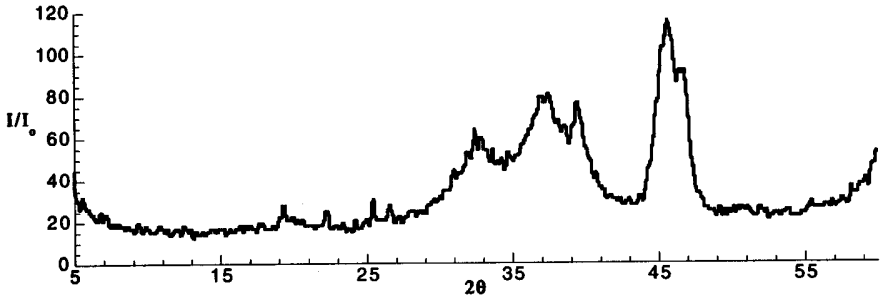

FIG. 11. Powder X-ray diffraction of Li(acac)/γ-alumina.

DRIFTS. Samples of Li/alumina were examined by DRIFTS to determine if any of the Li ions in the sample remained associated. Data for the four samples and the polycrystalline Li(acac) are shown in Fig. 10 [a, 58; b, 115; c, 150; d, 196 μmol Li/g alumina; e, polycrystalline Li(acac)]. All of the supported Li samples show absorbances at 1600, 1530, and 1410 cm^{-1} which are characteristic of the (acac) ligand chelated to Li ions. However, the slight shift upward in the vibration at 1537 cm^{-1} in spectra (a)–(d) from 1520 cm^{-1} in spectrum (e) suggest that the "breathing" vibration of the (acac) ligand in the supported samples is influenced by species present on the surface. We see no evidence of $Al(acac)_3$ in the DRIFT spectra as a major relaxation from the Al complex in not present in the spectra of the supported samples (24).

XRD. One of the samples (Li loading = 196 μmol Li/g alumina) was examined by XRD to determine the presence of polycrystalline metal complex. Small peaks are evident in the spectrum (Fig. 11) at 22.4° and 25.6° which correspond to peaks in the XRD of the neat Li(acac) at the d-spacing of 3.973 and 3.376 Å. Apparently, some reflections of polycrystalline Li(acac) are evident in this sample.

TGA—thermal decomposition. Thermal analysis of neat Li(acac) when heated in oxygen shows the loss of one (acac) ligand between 280 and 300°C (Fig. 12). The overall weight loss is less than that predicted by the following stoichiometry:

$$\text{Li(acac) (s)} \rightarrow \text{LiOH (s)} + \text{volatiles.}$$

The observed weight loss in this sample is 50% of the original weight, whereas, the predicted weight loss should be 77% of the original weight [(105.9 − 23.9)/105.9 × 100]. If we assume that the stoichiometry is explained by the formation of the oxide, then the predicted loss is 85.9%. Apparently, Li(acac) is difficult to decompose totally.

TGA—SO_2 adsorption. The adsorption of SO_2 is greatly improved for Li <50 μmol/g alumina over what is observed in the Mg/alumina sample. For Li loadings >50 μmol/g alumina the SO_2 adsorption is 0.12 mol/mol Li (Fig. 13). The dispersion of Li in these samples may be small as the expected incremental SO_2 adsorption is 0.5 mol/mol Li if *all* of the Li were available for adsorption assuming the SO_2 binds to the Li with the same stoichiometry as Li_2SO_4. The data were fit to give an intercept of 392 μmol SO_2/g alumina which is much greater than that for the bare alumina (265 μmol SO_2/g alumina). This increased SO_2 adsorption over that by the bare alumina may indicate the influence

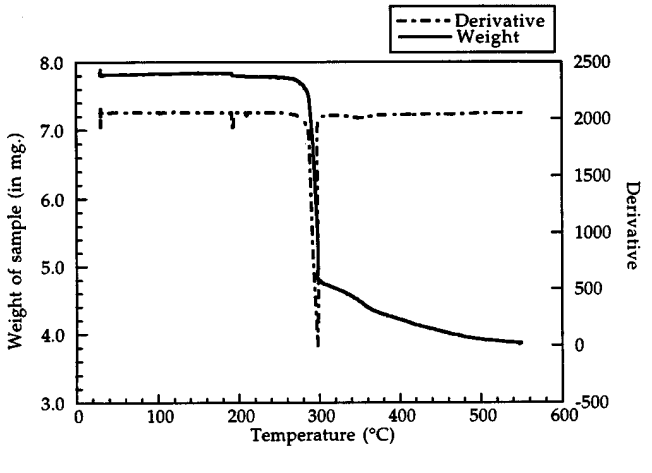

FIG. 12. Thermal gravimetric analysis of neat Li(acac).

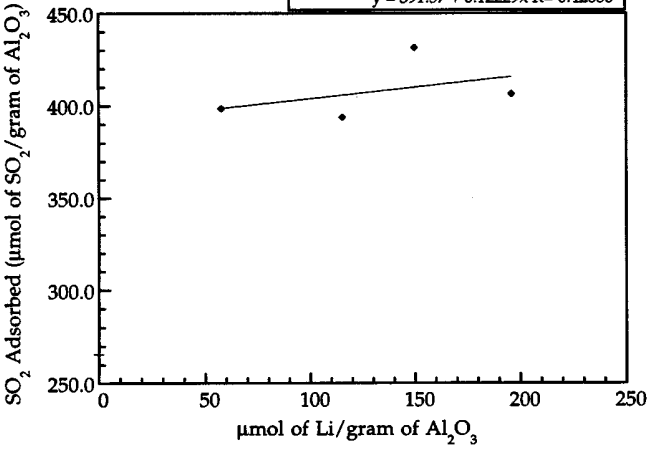

FIG. 13. SO_2 adsorption on Li(acac)/γ-alumina.

of Li on the surface to enhance the normal modes of SO_2 adsorption on the alumina. Such enhancing effect has been reported by others in the formation of surface sulfates on ceria-doped, high-alumina, cracking catalysts at high temperatures (29). The sulfate/ceria mole ratio in these catalysts was 100–300 for ceria doping levels of 5–20 ppm. The authors reported the ceria as having a "catalytic" effect on the sorption of SO_2. The lowest weight loadings of Li in our samples was 346 ppm which is much greater than that reported by the authors in the promoting effect of ceria.

DISCUSSION

We have presented data for alumina decorated with group IA and group IIA metal acetylacetonates. The maximum loading of $Mg(acac)_2$/alumina was 165 μmol/g alumina. We estimate the maximum loading of the complex by two models. One model assumes that the metal complexes pack on the surface as a 2-D layer in a close-pack arrangement. If the projected area of each complex is 58.76 $Å^2$ per molecule and the available surface area of the alumina is 150 m^2/g, then the monolayer loading of complexes is 412 μmole/g. The other model recognizes the structure of the alumina as described by Knözinger and Ratnasamy (13) who report a total OH site density of 14.5×10^{14} (OH/cm^2) for a sample which has not been dehydroxylated. Our alumina samples which are contacted with absolute methanol have not been heated above room temperature; thus, they may be considered as not dehydroxylated. The model for the B-layer of the (**111**) plane shows that the fraction of the surface having acidic protons (type III sites) is 0.25. This fraction when multiplied by the total OH site density gives a density of sites equals 3.6×10^{14} (OH/cm^2). Using the surface area of alumina gives an acid site density of 5.4×10^{20} OH sites/g alumina. This loading may be used to estimate the monolayer loading $Mg(acac)_2$ if we assume a stoichiometry of OH groups/$Mg(acac)_2$. We start with the minimum of 1 OH/acac or 2/molecule to give an estimate of the site density $= 2.7 \times 10^{20}$ $Mg(acac)_2$/g alumina $= 449$ μmole/g. The observed loading is less than either of the predicted loading for a monolayer, which suggests that only a fraction of the total surface (0.37–0.40) is covered by the metal complex.

The incremental SO_2 adsorption on the Mg/alumina was proportional to the moles of the decomposed metal complex on the alumina. It appeared that the total SO_2 adsorption in the sample was the sum of that originally in the sample and that added by the alkaline metal. This result is quite unexpected in that random decoration of the alumina surface would have suggested that some of the SO_2 adsorption sites in the sample must surely be covered with the adsorption of the complex from solution. We are left to conclude that the metal complex is selectively adsorbed on to those sites which do not adsorb SO_2. Candidates for such sites include surface hydroxyl groups not unlike those shown by Kenvin (21) as necessary to anchor $Cu(acac)_2$ on to silica. This OH group will show some acidic character in order to hydrogen bond to the (acac) ligand via the π electrons (21). Acidic OH groups are speculated to exist on the surface of γ-alumina as described in the models by Knözinger and Ratnasamy (13). Thus, we conclude that the (acac) ligands orchestrate the adsorption of the $Mg(acac)_2$ onto the surface of the alumina so that only acidic OH sites are used. Furthermore, we speculate that these sites are not involved in the sorption of SO_2 so that when the complexes are decomposed, new sites for SO_2 adsorption are created which merely add to the population of such sites.

This model for dispersing of the metal complex on the surface ensures isolation of the resulting metal oxide upon thermolysis of the complex. We find evidence of this high dispersion in the incremental SO_2 adsorption per Mg ion which is near unity initially and remains at that value for repeated heating and cooling cycles for temperatures to 500°C. The mechanism for SO_2 adsorption assumes that one SO_2 molecule adsorbs to one exposed surface Mg ion. Additional evidence of high dispersion comes from the absence of any XRD peaks characteristic of the metal complex prior to thermolysis. Kenvin showed that multilayers of the $Cu(acac)_2$/silica lead to polycrystalline CuO upon thermolysis of the complexes (30). As with the present adsorbents, Kenvin's catalysts which were developed from monolayer films of $Cu(acac)_2$/silica remained well-dispersed upon heating cycles to 450°C.

We speculate that the reversible adsorption of SO_2 to the Mg/alumina is a result of the well-dispersed Mg ions present in the sample. The observed adsorption capacity of 0.92 SO_2/Mg ion is consistent with a model for which each SO_2 molecule requires one site near/on a Mg ion. Heating of the sample causes the SO_2 to desorb so that the adsorption is reversible. A single sample of adsorbent can be put through SO_2 adsorption and desorption cycles without any loss of adsorption capacity which suggests to us that sulfate formation does not occur on these adsorbents as a result of the high dispersion of the Mg ions.

Li(acac) apparently dissociates partially into its ions upon solvation. Some of the undissociated metal complex reaches the surface of the alumina. We speculate that the fate of the undissociated Li(acac) is the same as the $Mg(acac)_2$; i.e., they attach to acidic OH groups where they will be partially decomposed upon heating to produce sites for SO_2 adsorption. The dissociated Li cations attach to other sites, such as basic OH or O anions. The effect of these Li cations is to enhance the basicity of the OH or O anions, therefore improving the ability of these alumina sites to chemisorb SO_2. We speculate that the effect of the cation is global in the sense that one Li cation may increase the basicity of several anionic neighbors in the surface lattice as the incremental SO_2 adsorption is >2 mol SO_2/mol Li for samples containing <50 μmol Li/g alumina.

The morphology of the Li on the surface is not well defined. The XRD data suggest that small crystallites of the Li(acac) may be present prior to thermolysis. Past experience suggest that multilayers of metal complexes lead to poorly dispersed metal oxides upon thermolysis (30). The incremental SO_2 adsorption (0.12 mol/mol Li) at Li loadings >50 μmol/g alumina suggests that not all the Li is available for sorption which confirms our earlier conclusions relating to poor dispersion of the Li ions.

CONCLUSIONS

We extended our previous results to produce another material having a thin film of a metal complex on an oxide support. This film of a group IIA metal acetylacetonate may be decomposed to produce a robust and well-dispersed metal oxide on alumina which shows enhanced SO_2 adsorption. The present technology allows us to selectively decorate a portion of the alumina surface which apparently does not participate directly with the SO_2 adsorption process. Such selective decoration of a surface may find usefulness in the preparation of a high efficiency adsorbent or catalyst.

The chemistry of the group IA acetylacetonates prevented us from fully exploiting the present technology to decorate the alumina selectively with a group IA metal ion. Apparently, the dissociation of Li(acac) leads to a surface covered in part with Li cations and undissociated Li(acac). The ionic nature of the Li(acac) probably frustrated the self-assembling features of the (acac) ligands in a chelated metal acetylacetonate so that the Li(acac) is present on the alumina in multilayers prior to thermolysis. The resulting LiO residue was not well dispersed. The SO_2 adsorption properties are somewhat better than the MgO/alumina at metal loadings <150 μmol/g alumina; however, the utilization of the incremental alkali is poorer in the LiO/alumina at higher metal loadings.

ACKNOWLEDGMENTS

The authors acknowledge the support from the U.S. Department of Energy; Pittsburgh Energy Technology Center through Contract DE-FG-22-90PC90292 and from the Georgia Institute of Technology through the Focused Research Program in Surface Science and Catalysis. We also acknowledge the helpful discussions with Professor J. Aaron Bertrand, School of Chemistry and Biochemistry, Georgia Institute of Technology (Atlanta, GA).

REFERENCES

1. Slack, A. V., "Sulfur Dioxide Removal from Waste Gases." Noyes Data Corporation, 1971.
2. Gavalas, G. R., Edelstein, S., Glytzani-Stephanolpoulos, M., and Weston, T. A., *Am. Inst. Chem. Eng.* **33**(2), 258 (1987).
3. Pollack, S. S., Chisholm, W. P., Obermyer, R. T., Hedges, S. W., Ramanathan, M., and Montano, P. A., *Ind. Eng. Chem. Res.* **27**, 2276 (1988).
4. Yoo, J. S., Bhattacharyya, A. A., and Radlowski, C. A., *Ind. Eng. Chem. Res.* **30**, 1444 (1991).
5. Knözinger, H., *Adv. Catal.* **25**, 184 (1976).
6. van Cauwelaert, F. H., and Hall, W. K., *Trans. Faraday Soc.* **66**, 454 (1970).
7. Hightower, J. W., and Hall, W. K., *Trans. Faraday Soc.* **66**, 477 (1970).
8. Peri, J. B., *J. Phys. Chem.* **70**, 3168 (1966).
9. Pines, H., and Manassen, J., *Adv. Catal.* **16**, 49 (1966).
10. MacIver, D. S., Wilmot, W. H., and Bridges, J. M., *J. Catal.* **3**, 502 (1964).
11. Peri, J. B., *J. Phys. Chem.* **69**, 220 (1965).
12. Dabrowski, J. E., Butt, J. B., and Bliss, H., *Catal.* **18**, 297 (1970).
13. Knözinger, H., and Ratnasamy, P., *Catal. Rev.—Sci. Eng.* **17**(1), 31 (1978).
14. Deo, A. V., Dalla Lana, I. G., and Habgood, H. W., *J. Catal.* **21**, 270 (1971).
15. Datta, A., Cavell, R. G., Tower, R. W., and George, Z. M., *J. Phys. Chem.* **89**, 443 (1975).
16. Chang, C. C., *J. Catal.* **53**, 374 (1978).
17. Saur, M., Bensitel Mohammed Saad, A. B., Lavalley, J. C., Tripp, C. P., and Morrow, B. A., *J. Catal.* **99**, 104 (1986).
18. Glass, R. W., and Ross, R. A., *Can. J. Chem.* **50**, 2537 (1972).
19. Karge, H. G., and Dalla Lana, I. G., *J. Phys. Chem.* **88**, 1538 (1984).
20. Haslbeck, L. G., Neal "Technical Evaluation of the NOXSO Combined NO_x/SO_2 Flue Gas Treatment Process," American Institute of Chemical Engineers Spring National Meeting, Houston, TX, March 24–28, 1985.
21. Kenvin, J. C., White, M. G., and Mitchell, M. B., *Langmuir* **7**, 1198 (1991).
22. White, E., *J. Chem. Soc.* 1413 (1928).
23. Babb, K. H., and White, M. G., *J. Catal.* **98**, 343 (1986).
24. Lawson, K. E., *Spectrochim. Acta* **17**, 248–2158 (1961).
25. van Veen, J. A., Robert, *J. Colloid Interface Sci.* **21**(1), 214 (1988).
26. Mitchell, Mark, B., Chakravarthy, Vasumathi, R., and White, Mark, G., *Langmuir* **10**, 4523–4529 (1994).
27. Gurevich, M. Z., Sas, T. M., Lebedeva, N. E., Zelentsov, V. V., and Stepin, B. D., *Russ. J. Inorg. Chem.* **17**(4), 556 (1972).
28. Decanio, E. C., Nero, V. P., and Bruno, J. W., *J. Catal.* **135**, 444 (1992).
29. Bertolacini, R. J., Hirschberg, E. H., and Modica, F. S., U.S. patent 4,423,019 (1983).
30. Kenvin, J. C., and White, M. G., *J. Catal.* **130**, 447 (1991).